atmosphere

Article

A Comparative Investigation of the Characteristics of Nocturnal Ozone Enhancement Events and Their Effects on Ground-Level Ozone and $PM_{2.5}$ in the Central City of the Yellow River Delta, China, in 2022 and 2023

Cong An [1], Yongxin Yan [1], Xiaoshuai Gao [1], Xiaoyu Yan [1,2], Yuanyuan Ji [1], Fanyi Shang [3], Jidong Li [3], Luyao Tan [4], Rui Gao [1], Fang Bi [1] and Hong Li [1,*]

1 State Key Laboratory of Environmental Criteria and Risk Assessment, Chinese Research Academy of Environmental Sciences, Beijing 100012, China; ancong_22@163.com (C.A.); yyx_in@163.com (Y.Y.); s202265286@emails.bjut.edu.cn (X.G.); yanxiaoyu22@mails.jlu.edu.cn (X.Y.); ji.yuanyuan@craes.org.cn (Y.J.); gaorui@craes.org.cn (R.G.); bifang@craes.org.cn (F.B.)
2 College of Earth Sciences, Jilin University, Changchun 130061, China
3 Dongying Ecological and Environmental Bureau, Dongying 257091, China; dyhbsfy@126.com (F.S.); shbjzlb@dy.shandong.cn (J.L.)
4 Ltd. of Shandong Environmental Protection Industry Corp., Jinan 250061, China; tanluyyy@163.com
* Correspondence: lihong@craes.org.cn

Abstract: In recent years, nocturnal ozone enhancement (NOE) events have emerged as a prominent research focus in the field of the atmospheric environment. By using statistical analysis methods, we conducted a comparative investigation of nocturnal ozone concentrations and NOE events in Dongying, the central city of the Yellow River Delta, China, in 2022 and 2023, and further explored the effects of NOE events on O_3 and $PM_{2.5}$ on the same night and the subsequent day. The results showed that from 2022 to 2023, in Dongying, the annual average nocturnal ozone concentrations increased from 51 $\mu g/m^3$ to 59 $\mu g/m^3$, and the frequency of NOE events was higher in the spring, summer, and autumn, and lower in the winter. The NOE events not only exhibited promoting effects on nocturnal O_3 and O_x, and on the daily maximum 8 h average concentration of O_3 (MDA8-O_3) on the same day (comparatively noticeable in summer and autumn), but also demonstrated a clear impact on nocturnal $PM_{2.5}$ and $PM_{2.5}$-bounded NO_3^- and SO_4^{2-} (especially in winter). Additionally, the NOE events also led to higher concentrations of O_3 and O_x, as well as higher MDA8-O_3 levels during the subsequent day, with more observable impacts in the summer. The results could strengthen our understanding about NOE events and provide a scientific basis for the collaborative control of $PM_{2.5}$ and O_3 in urban areas in the Yellow River Delta in China.

Keywords: nocturnal ozone (O_3); $PM_{2.5}$; effect; secondary pollution; the Yellow River Delta

check for updates

Citation: An, C.; Yan, Y.; Gao, X.; Yan, X.; Ji, Y.; Shang, F.; Li, J.; Tan, L.; Gao, R.; Bi, F.; et al. A Comparative Investigation of the Characteristics of Nocturnal Ozone Enhancement Events and Their Effects on Ground-Level Ozone and $PM_{2.5}$ in the Central City of the Yellow River Delta, China, in 2022 and 2023. *Atmosphere* **2024**, *15*, 475. https://doi.org/10.3390/atmos15040475

Academic Editors: Antonio Donateo, Jinhui Gao, Kaihui Zhao and Yonghua Wu

Received: 31 January 2024
Revised: 15 March 2024
Accepted: 2 April 2024
Published: 11 April 2024

1. Introduction

Ground-level ozone (O_3) is mainly produced by precursors such as nitrogen oxides (NOx) and volatile organic compounds (VOCs) under light conditions [1–5]. Due to the synthetic effects of photochemical generation, dry depositions, and boundary layer entrainment, the diurnal variation in ozone concentration usually presents a unimodal distribution; that is, the concentration is higher during the daytime and lower at nighttime, which has been confirmed by a large number of field observations [6–11]. However, in recent years, many studies have demonstrated that nocturnal ozone concentrations are surging and that a nocturnal ozone peak occurs, which has been widely observed in the United States, Europe, and China [12–19]. Studies have reported that higher nocturnal ozone concentrations may have an impact on atmospheric chemical processes, human health, and vegetation growth [15,20–22]. Wang et al. suggested that the increase in nocturnal ozone concentrations in China in recent years has led to an increase in the nocturnal atmospheric oxidation capacity in China [21]. Agathokleous et al. believed that nocturnal ozone enhancement may adversely affect plant and animal growth [18,23]. Therefore, it becomes imperative to conduct comprehensive research elucidating the phenomenon of nocturnal ozone enhancement (NOE).

Currently, numerous studies have been conducted to investigate the characteristics and underlying causes of NOE. He et al. [14] found that the average annual frequency of NOE events ranged from 28% to 41% in China, the United States, and the European Union, and that the frequency of NOE events in China is significantly higher than that in the United States and the European Union. Wu et al. [24] studied the NOE events and their causes in the Pearl River Delta, China and found that the annual average frequency of NOE events is 53 days per year and the average nocturnal ozone peak is 58 $\mu g/m^3$. The low-level jet stream is the main meteorological process that triggers the NOE events, accounting for an average of 61%, and convective storms account for about 11%. In addition, sea–land breezes and mountain–valley circulation, typhoons, and stratospheric ozone intrusions also contribute to NOE events [25–29]. Few studies have speculated on the chemical effects of NOE events. Wu et al. preliminarily explored the relationship between nocturnal ozone concentration and the daily maximum 8 h average concentration of O_3 (MDA8-O_3) of the following day and found that there was a good correlation between them [24]. He et al. [30] suggested that the NOE would lead to a persistently high value of 8 h average ozone concentration from night to the early next morning. He et al. [31] found that nocturnal $PM_{2.5}$ concentrations and odd oxygens (O_x = NO_2 + O_3) are obviously higher during NOE events in the Pearl River Delta region of China than during non-nocturnal ozone enhancement (NNOE) events. Currently, a dearth of investigations exists concerning the effects of NOE on secondary pollutants. Furthermore, there is a notable paucity of detailed analyses, particularly in discerning the interannual and monthly scale influences of NOE on secondary pollutants. Most of the current studies focus on the developed regions of China, such as the North China Plain and the Pearl River Delta, with limited research attention directed towards the Yellow River Delta.

Dongying is a central city of China's Yellow River Delta, bordered by the Bohai Sea to the east and north. In recent years, the air quality in Dongying has improved significantly, but the problem of ozone pollution is still prominent [32–34]. An et al. found that the nocturnal ozone concentration increased in Dongying from 2017 to 2022, and the average nocturnal ozone concentration in the ozone pollution season in 2022 increased by 12 $\mu g/m^3$ compared with 2017, which was greater than the increase during the daytime, suggesting an increase in the nocturnal atmospheric oxidation capacity in this region [35]. Furthermore, the Yellow River Delta in China has experienced frequent NOE events, exemplified by the night of 17 June 2022. During this specific event, despite the presence of thundershowers, the ozone concentration persisted at elevated levels, characterized by three distinct increases. Nevertheless, a comprehensive and systematic analysis of the characteristics of NOE events in Dongying is currently absent. Hence, it is imperative to examine the characteristics of the NOE events and their influence on O_3 and $PM_{2.5}$ in Dongying.

Based on the data of normal pollutants and $PM_{2.5}$ components concentrations in Dongying, a central city of the Yellow River Delta, China, this study analyzed the characteristics of nocturnal ozone concentration and NOE events in Dongying and further explored the effects of NOE events on the concentrations of O_3, O_x, $PM_{2.5}$, nitrate (NO_3^-), sulfate (SO_4^{2-}), and secondary organic carbons (SOC) at night and the following day. The research findings are helpful to understand the characteristics of nocturnal ozone concentration and the NOE events in the Yellow River Delta and to clarify the impact of NOE events on secondary pollutants. This research contributes to a strengthened understanding of NOE events and provides a scientific foundation for the collaborative control of $PM_{2.5}$ and O_3 in urban areas in the Yellow River Delta, China.

2. Materials and Methods

2.1. Observation Period and Location

Dongying, located in the northern part of Shandong Province in China and bordered by the Bohai Sea to the east and north, is an important passage to the sea in the Yellow River Basin and a central city of the Yellow River Delta, China [36]. The hourly concentration data of normal pollutants (O_3, SO_2, NO_2, and $PM_{2.5}$), $PM_{2.5}$-bounded ionic components, organic carbon (OC), and elemental carbon (EC) used in this study were obtained from the Dongying Atmospheric Observatory ("Atmospheric Observatory", Figure 1) (http://117.78.41.74:9830/, (accessed on 10 March 2024)). The investigation spanned from 1 January 2022 to 31 December 2023. The Atmospheric Observatory is mainly surrounded by residential areas and commercial office areas, with convenient transportation and no obvious industrial pollution sources, which can accurately reflect the air pollution situation in Dongying (Figure 1). All the observation items were continuously monitored using automatic monitoring devices, among which the SO_2, NO-NO_2-NOx, and O_3 were monitored with 43i, 42i, and 49i (Thermo Fisher Scientific Inc., Waltham, MA, USA), respectively. Particulate matters were monitored online with BAM1020 (Met One Instruments Inc., Washington, DC, USA). The ion component analyzer model was S−611EG (Zhang Jia Ltd., Taiwan, China) and the OC and EC analyzer model was OCEC-100 (Focused Photonics Inc., Hangzhou, Zhejiang, China).

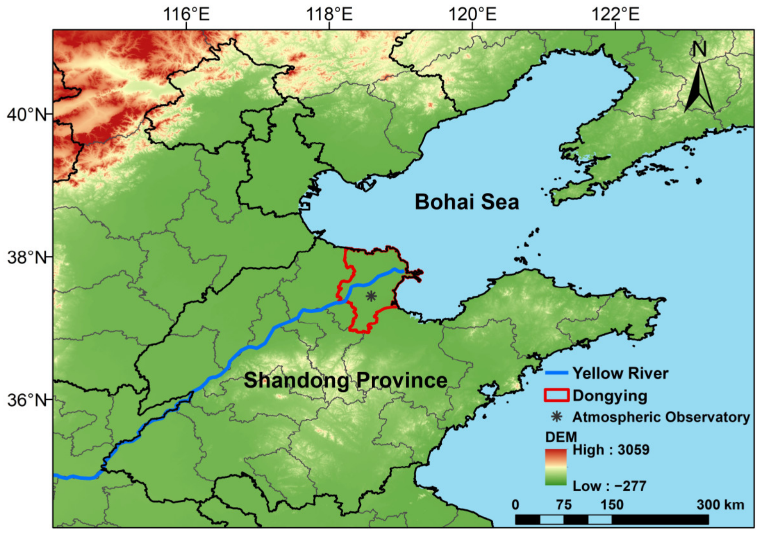

Figure 1. Geographic location of Dongying City.

2.2. Relevant Definitions

Daytime and nighttime are generally defined based on the characteristic variations in solar radiation. Numerous studies have utilized methods such as machine learning and regression models to estimate the features of solar radiation in China and globally [37–43], with solar radiation characteristics potentially varying across different regions. Consequently, the ultraviolet radiation characteristics in Dongying were analyzed. Negligible ultraviolet radiation levels were observed from 0:00 to 6:00 and from 20:00 to 23:00 (Figure 2). Therefore, the period from 20:00 to 6:00 of the next day is considered to be the nighttime of Dongying [14,35].

Nocturnal ozone enhancement events (NOE events): Based on the definitions of NOE events in previous studies [14,24,31], NOE events are defined as the ozone concentration increases by more than 10 $\mu g/m^3$ in two successive hours of a given night (20:00 to 06:00 of the next day), and the corresponding nocturnal maximum O_3 concentration is called the nocturnal ozone peak.

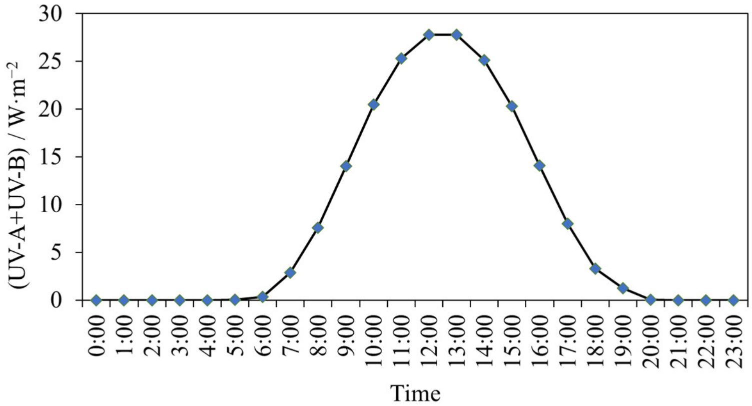

Figure 2. Dinunal variations in ultraviolet radiation in Dongying from 2022 to 2023.

Non-nocturnal ozone enhancement events (NNOE events): NNOE events are defined as no increases in nocturnal ozone or increases of less than 10 μg/m^3 in two successive hours of a given night (20:00 to 06:00 of the next day).

2.3. Data Processing

2.3.1. Annual Frequency of NOE Events

The annual frequency of NOE events is calculated as the proportion of nights with NOE events occurring relative to the total number of nights in a year. Mathematically, it can be expressed as follows:

$$\text{Annual frequency of NOE events} = \frac{\text{Number of nights with NOE events}}{\text{Total number of nights in a year}} * 100\%, \quad (1)$$

The monthly frequency of NOE events is calculated as the proportion of nights with NOE events occurring relative to the total number of nights in a month. Mathematically, it can be expressed as follows:

$$\text{Monthly frequency of NOE events} = \frac{\text{Number of nights with NOE events}}{\text{Total number of nights in a month}} * 100\%, \quad (2)$$

2.3.2. Transformation Rate of Nitrates and Sulfates

In this study, the transformation rate of nitrates (NOR) and the transformation rate of sulfates (SOR) were used to determine the transformation status of gaseous precursors such as NO_2 and SO_2 to form secondary inorganic ions [34,44]. The higher the values of NOR and SOR, the higher the degree of secondary transformation of NO_2 and SO_2 in the atmosphere. The equations are as follows:

$$\text{NOR} = N_1/(N_1 + N_2), \quad (3)$$

$$\text{SOR} = S_1/(S_1 + S_2), \quad (4)$$

where N_1 and N_2 represent the concentration of NO_3^- and NO_2, respectively, in mol/m^3; and S_1 and S_2 represent the concentration of SO_4^{2-} and SO_2, respectively, in mol/m^3.

2.3.3. Calculation of Secondary Organic Carbon

In this study, the OC/EC ratio method was used to calculate the mass concentration of SOC [34,44]. The formula is as follows:

$$\text{SOC} = \text{OC} - \text{EC} \times (\text{OC}/\text{EC})_{\text{min}}, \quad (5)$$

where SOC represents secondary organic carbon in μg/m^3, OC and EC represent organic carbon and elemental carbon, respectively, and $(OC/EC)_{min}$ is the minimum value of OC/EC during the observation period.

3. Results and Discussion

3.1. Characteristics of Nocturnal Ozone Concentration in Dongying

3.1.1. Inter-Annual and Inter-Monthly Variations

From 2022 to 2023, the annual average nocturnal ozone concentration increased from 51 μg/m^3 to 59 μg/m^3 in Dongying (Figure 3). In addition, the results of the non-parametric test (Wilcoxon signed rank test) showed the statistics Z = −12.75009, $p < 0.05$, indicating that the nocturnal ozone concentration in 2023 was significantly higher than that in 2022.

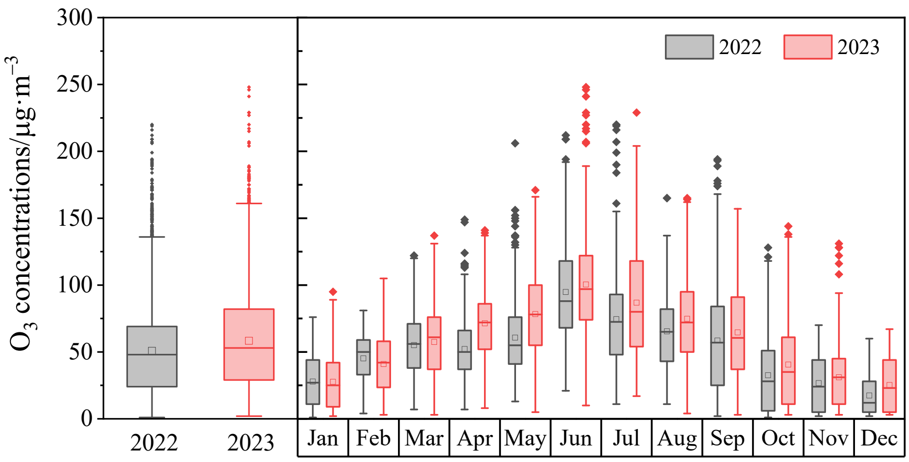

Figure 3. Inter-annual and inter-monthly changes in nocturnal ozone concentrations in Dongying from 2022 to 2023.

From 2022 to 2023, the monthly variation in nocturnal ozone concentration in Dongying showed a unimodal distribution, with the peak occurring in June (Figure 3). During January, February, October, and December, nocturnal ozone concentrations were relatively low, with monthly averages ranging from 17 to 45 μg/m^3. In contrast, from March to September, the nocturnal ozone concentrations were higher, with monthly averages ranging from 52 to 100 μg/m^3. This was consistent with the monthly variations in MDA8-O_3 in Dongying, which showed that the ozone concentration was higher in the ozone pollution season (from April to September), while the ozone concentration was lower in the non-ozone pollution season (other months) [35]. It can also be observed that the ozone levels in Dongying during nighttime and daytime exhibit relatively similar monthly variations (Figures 3–5). This finding is also supported by research by He et al. (2022). The nocturnal ozone concentration was higher in the ozone pollution season and lower in the non-ozone pollution season, indicating that the nocturnal ozone concentration was closely related to the daytime ozone pollution.

The nocturnal ozone concentrations from February to December 2023 were higher than those in 2022, and the most obvious increases were in April to May and July, with an increase of 12–19 μg/m^3 (Figure 3). The increase in nocturnal ozone concentration in Dongying in the past two years suggests that attention should be paid to the increase in nocturnal ozone concentration in the Yellow River Delta, which may alter the nighttime atmospheric oxidation capacity and further affect atmospheric chemical reactions.

The different percentiles of the nocturnal ozone hourly concentrations increased in Dongying from 2022 to 2023 (Figure 6). Compared to 2022, the nocturnal ozone concentrations increased at different percentiles in 2023 from high to low as follows: 15 μg/m^3 (95th percentile), 13 μg/m^3 (75th percentile), 5 μg/m^3 (50th and 25th percentiles), 4 μg/m^3 (99th percentile), and 1 μg/m^3 (5th percentile). It can be seen that the high and middle percentiles of the nocturnal ozone concentration increased most obviously in Dongying from 2022 to 2023. The increase in nocturnal ozone concentrations in Dongying is similar to the results of Li et al. (2023), who found that nocturnal ozone concentrations increased in most regions of China in the summer of 2019 compared to 2015, which was mainly caused by a reduction in both the ambient NO_2 concentration and wet scavenging in recent years [15].

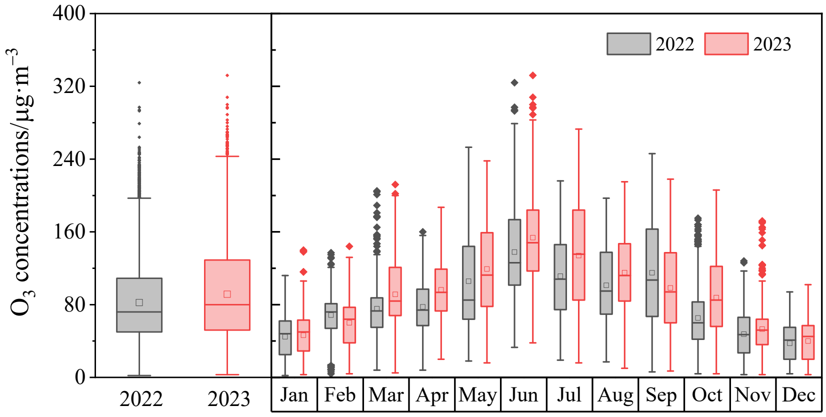

Figure 4. Inter-annual and inter-monthly changes in daytime ozone concentrations in Dongying from 2022 to 2023.

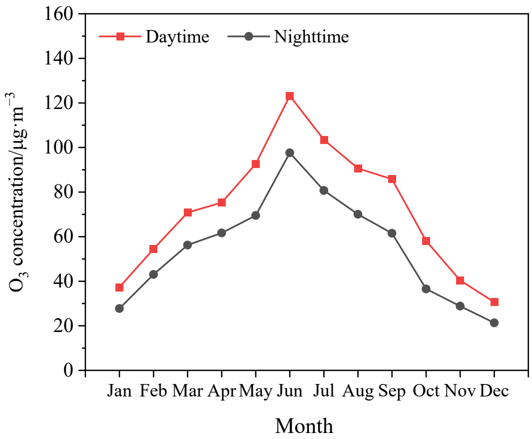

Figure 5. Monthly mean value changes in daytime and nighttime ozone concentrations in Dongying from 2022 to 2023.

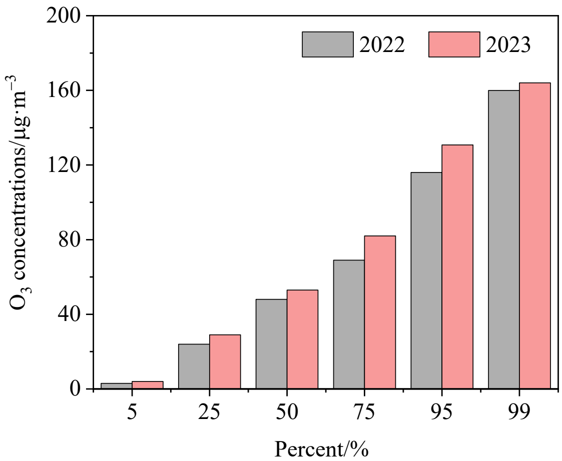

Figure 6. Characteristics of different percentiles of nocturnal ozone concentrations in Dongying from 2022 to 2023.

3.1.2. Diurnal Variation

From 2022 to 2023, the diurnal variation in nocturnal ozone concentration showed a decreasing trend or weak unimodal distribution in Dongying (Figure 7). The diurnal variation s in nocturnal ozone concentration during the ozone pollution season (April to September) showed a noticeable decreasing trend, while the diurnal variations from January to February and November to December showed a weak, unimodal distribution. Most of the nocturnal ozone concentrations increased slightly from 1:00 to 6:00. Compared with 2022, the nocturnal ozone concentration in Dongying increased from April to November in 2023. The most notable escalation was observed in July, characterized by an average elevation of 25 $\mu g/m^3$ from 20:00 to 21:00. Subsequently, a discernible rise was documented from 21:00 to 1:00 of the subsequent day in April, exhibiting an average increase of 21 $\mu g/m^3$. In May, a notable increase was noted from 20:00 to 0:00, demonstrating an average elevation of 20 $\mu g/m^3$. Following this, December's 2:00 to 6:00 timeframe showed an average increase of 20 $\mu g/m^3$, while October's 20:00 to 22:00 timeframe manifested an average rise of 19 $\mu g/m^3$. This may be due to the higher daytime ozone concentration in Dongying in 2023. The 90th percentile of MDA8-O_3 was 221 $\mu g/m^3$ in Dongying in July 2023, with an increase of 30 $\mu g/m^3$ compared with 2022. Higher ozone concentrations during the day in July 2023 may lead to higher ozone concentrations at night.

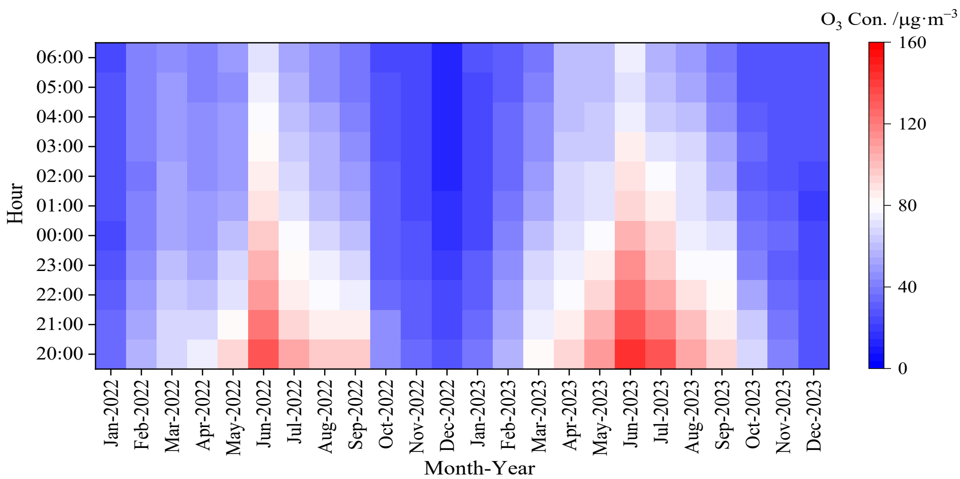

Figure 7. Diurnal variations in nocturnal ozone concentrations in Dongying from 2022 to 2023.

3.2. Characteristics of Nocturnal Ozone Enhancement Events in Dongying

3.2.1. Frequency Characteristics

NOE events in Dongying from January 1, 2022 to December 31, 2023 were selected. The results showed that the annual average frequency of NOE events was 44% and 43% in Dongying in 2022 and 2023, respectively. This is comparable to the results of He et al.'s research on the frequency of NOE events in China [14]. The NOE events may be attributed to the nocturnal transport of high ozone concentrations from upwind cities, the downward transport of ozone from the night residual layer, and some specific meteorological processes, such as low-level jet streams, convective storms, and local circulation [14,24–27,45,46]. Overall, the frequency of NOE events in Dongying was higher in spring, summer, and autumn and lower in winter from 2022 to 2023 (Table 1 and Figure 8). The frequency of NOE events from February to March, May, July, September, and November in 2023 decreased compared with 2022, while the frequency in January, April, June, August, October, and December in 2023 increased compared with 2022, and the largest increase was in August and October. This might be related to changes in pollutant emissions and meteorological conditions in Dongying.

Table 1. Frequency of NOE events in different months in 2022 and 2023 in Dongying.

	2022	**2023**
January	29%	32%
February	46%	36%
March	58%	55%
April	43%	47%
May	55%	42%
June	47%	53%
July	32%	23%
August	39%	58%
September	63%	47%
October	42%	61%
November	47%	33%
December	23%	32%

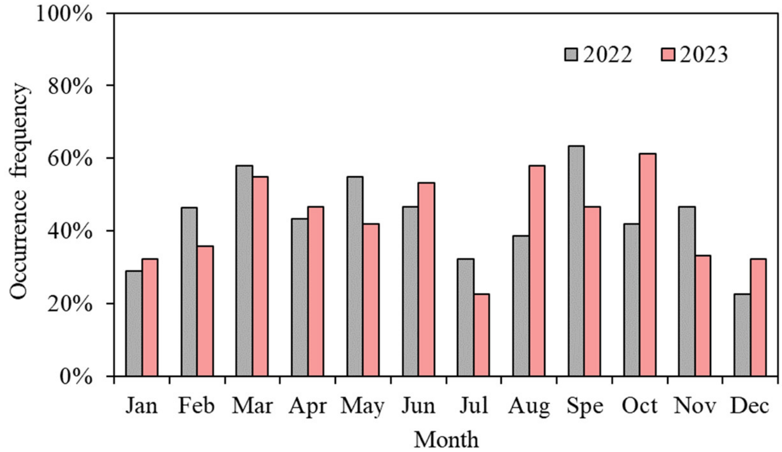

Figure 8. The frequency of NOE events in Dongying across different months from 2022 to 2023.

In particular, the frequency of NOE events in both July and December was relatively low. He et al. (2022) found that in the North China Plain, China, the frequency of NOE events is higher in the warm season and lower in the cold season, consistent with the seasonal variation characteristics of daytime ozone concentrations [14]. Hence, the daytime ozone concentration appears to influence the frequency of NOE events to a certain extent. The ozone concentration in Dongying is relatively low in December (Figures 3 and 4), corresponding to a lower frequency of NOE events, aligning with findings from He et al. (2022). However, in July, despite higher ozone concentrations (Figures 3 and 4), the frequency of NOE events is lower, which may be influenced not only by the daytime ozone concentration but also by factors such as transport and atmospheric stability [47]. Atmospheric stability is typically influenced by various factors such as seasonality, geographical location, and meteorological conditions. The nocturnal boundary layer height serves as a robust indicator of the nocturnal atmospheric vertical mixing capability. Thus, the average ozone concentrations and nocturnal boundary layer heights in Dongying for different months were analyzed to ascertain the reasons behind the lower occurrence frequency of NOE events in July and December. A higher nocturnal boundary layer height indicates more vigorous vertical mixing processes, which are conducive to ozone vertical transport. Conversely, a lower nocturnal boundary layer height implies relatively stable atmospheric conditions [48]. During the study period, the average ozone concentrations were higher in July (103.5 $\mu g \cdot m^{-3}$) and lowest in December (30.6 $\mu g \cdot m^{-3}$) (Figure 9a). The lowest nocturnal boundary layer height was recorded in July (519.8 m), with December exhibiting relatively lower boundary layer heights (589.0 m), indicating relatively stable atmospheric conditions in both July and December (Figure 9b). Therefore, the lower nocturnal boundary layer heights and higher ozone concentrations in July contributed to the lower frequency of NOE events in July, while the lower nocturnal boundary layer heights and lower ozone concentrations in December led to the reduced frequency of NOE events in December. This suggests that, compared to ozone concentrations, the nocturnal boundary layer height may play a more crucial role in the occurrence of NOE events in Dongying.

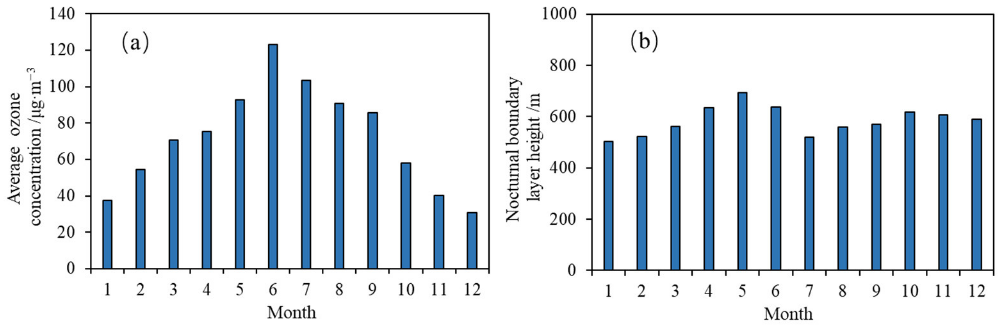

Figure 9. Monthly distribution characteristics of (**a**) average ozone concentration and (**b**) nocturnal boundary layer height in Dongying from 2022 to 2023.

Compared with 2022, the frequency of NOE events at 22:00, 23:00, 1:00, and 3:00 in 2023 decreased, while the frequency at 0:00, 4:00, and 6:00 increased (Figure 10). Overall, the frequency of NOE events was the highest at 2:00 in Dongying, with a total of 66 events during the two years, followed by 3:00, 4:00, and 6:00. The distribution characteristics of NOE events in Dongying at different times in 2022 and 2023 were generally similar. The frequency of NOE events was higher between 2:00 and 4:00, while it was lower between 21:00 and 1:00 the next day. The NOE events exhibited a higher frequency around midnight and a lower frequency in the early night hours. This pattern may be attributed to the stronger NOx titration effects shortly after sunset, making NOE events less likely to occur during the early night hours [14,24,46].

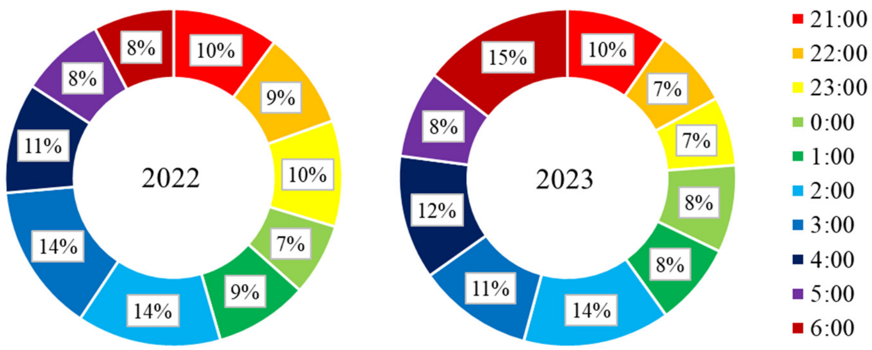

Figure 10. The frequency of NOE events in Dongying at different times from 2022 to 2023.

3.2.2. Characteristics of Nocturnal Ozone Peak and Ozone Increase Magnitude

The nocturnal ozone peak is most frequently distributed in the range of 40–60 μg/m^3 (occurring 125 times), followed by 20–40 μg/m^3 (occurring 99 times), 60–80 μg/m^3 (occurring 91 times), and 80–100 μg/m^3 (occurring 67 times) (Figure 11a). During the study period, the nocturnal ozone peak exceeded 160 μg/m^3 on six occasions, and the maximum nocturnal ozone peak was 210 μg/m^3. This is comparable to the maximum of nocturnal ozone peaks in Jinan, China, Shenzhen, China, and Malaysia [45–47,49,50]. It could be seen that Dongying, a central city of the Yellow River Delta, had extremely high nocturnal ozone peaks when NOE events occurred, which might have adverse effects on human health.

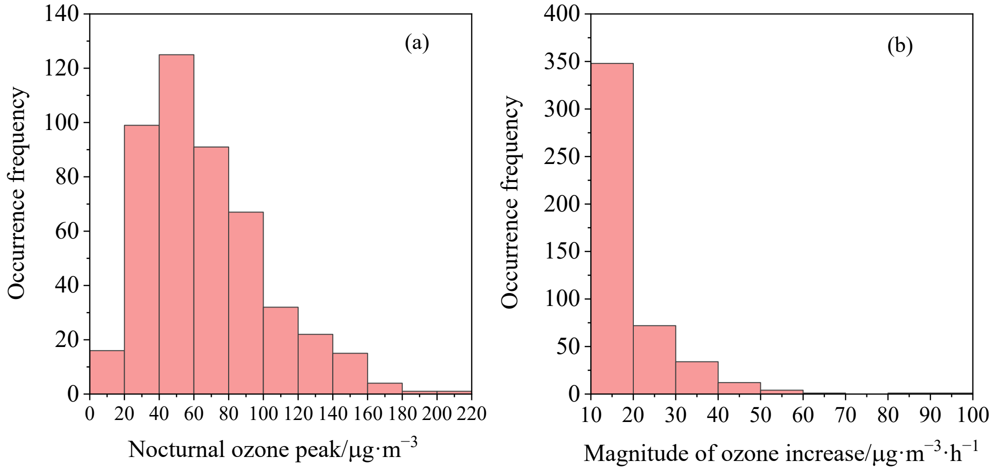

Figure 11. Distribution characteristics of (**a**) nocturnal ozone peak and (**b**) magnitude of ozone increase in Dongying from 2022 to 2023.

In the majority of NOE events in Dongying from 2022 to 2023, the ozone increase magnitude ($\Delta O_3/\Delta t$) was distributed in the range of 10 to 20 μg/m^3, followed by 20 to 30 μg/m^3, 30 to 40 μg/m^3, and 40 to 50 μg/m^3 (Figure 11b). This is consistent with the results of He et al. [14], which showed that the majority of nocturnal ozone that increased in magnitude in China ranged from 10 to 20 μg/m^3. The maximum increase in nocturnal ozone concentration in Dongying can reach up to 95 μg/m^3. Currently, most studies generally believe that NOE events are caused by horizontal advection and vertical transport. When extreme weather conditions occur, such as typhoons and strong convective weather, nocturnal ozone concentrations may experience significant increases [26,51,52]. Therefore, the magnitude of nocturnal ozone increase is primarily distributed in the low concentration range, with fewer occurrences in the high concentration range, possibly due to the infrequency of extreme weather events under normal circumstances.

From 2022 to 2023, the nocturnal ozone peak in Dongying gradually decreased from 21:00 to 6:00 of the next day (Figure 12). During the study period, the nocturnal ozone peak was higher from 21:00 to 23:00, with an average value of 81 μg/m^3. From 0:00 to 6:00, the nocturnal ozone peak changed slightly, and the average nocturnal ozone peak was 60 μg/m^3. This is consistent with the results of Wu et al.'s research in the Pearl River Delta in China, which showed a gradual decreasing trend in nocturnal ozone peak from 21:00 to 6:00 of the next day [24].

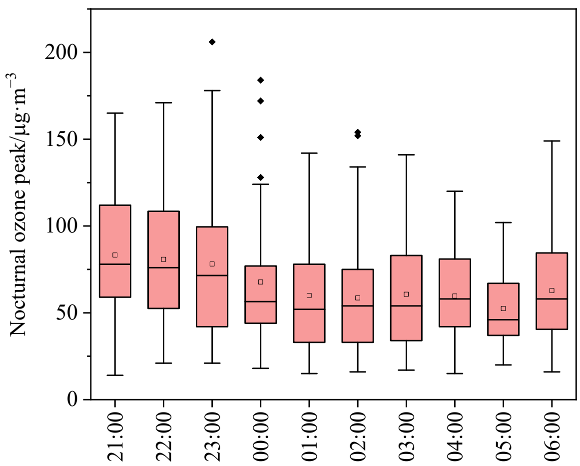

Figure 12. Distribution characteristics of nocturnal ozone peaks at different times in Dongying from 2022 to 2023.

3.3. Effects of Nocturnal Ozone Enhancement Events on Ozone and $PM_{2.5}$ Concentrations in Dongying

3.3.1. Diurnal Variations in Ozone and Other Air Pollutants during Different Seasons

The gas and aerosol component concentrations in Dongying during different seasons from 2022 to 2023 are shown in Figures 13 and 14. The daily variations in O_3 concentrations in different seasons exhibited a single-peak distribution, with peak values of 119 μg/m^3 (at 16:00), 150 μg/m^3 (at 16:00), 108 μg/m^3 (at 15:00), and 70 μg/m^3 (at 15:00) during the different seasons. The daily variation in $PM_{2.5}$ concentrations showed a fluctuating trend, with higher concentrations in the morning and night, reaching maximum values of 50 μg/m^3 (at 9:00), 33 μg/m^3 (at 9:00), 48 μg/m^3 (at 9:00), and 66 μg/m^3 (at 10:00) in different seasons. The daily variations in NO_2 concentrations followed a U-shaped pattern, with higher concentrations in the morning and night, reaching maximum values of 30 μg/m^3 (at 8:00), 21 μg/m^3 (at 8:00), 41 μg/m^3 (at 8:00), and 40 μg/m^3 (at 8:00) during the different seasons. The SO_2 concentrations exhibited relatively gentle daily variation characteristics, with a weak peak around noon, reaching maximum values of 15 μg/m^3 (at 11:00), 8 μg/m^3 (at 11:00), 12 μg/m^3 (at 10:00), and 19 μg/m^3 (at 10:00) during the different seasons.

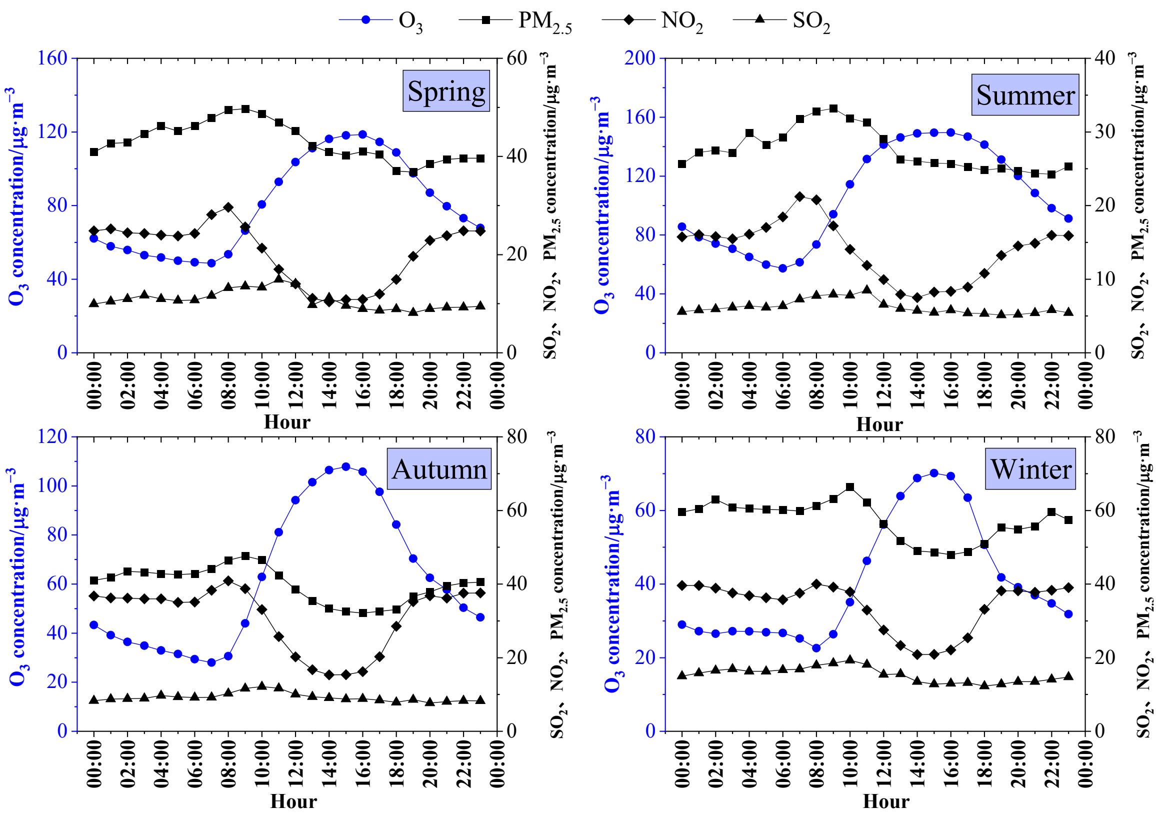

Figure 13. Distribution characteristics of O_3, $PM_{2.5}$, NO_2, and SO_2 concentrations in Dongying during different seasons from 2022 to 2023.

The daily variations in O_x concentrations also showed a single-peak distribution, with peak values of 129 μg/m^3 (at 16:00), 156 μg/m^3 (at 16:00), 121 μg/m^3 (at 16:00), and 90 μg/m^3 (at 16:00) during the different seasons. The $PM_{2.5}$-bounded NO_3^- concentrations in the spring, summer, and autumn exhibited distinct daily variations, with higher concentrations in the early morning and night and lower concentrations in the afternoon, reaching peak values of 15 μg/m^3 (at 8:00), 9 μg/m^3 (at 7:00), and 15 μg/m^3 (at 9:00). In winter, the NO_3^- concentrations showed a relatively gradual daily variation, with a peak value of 16 μg/m^3 (at 11:00). The $PM_{2.5}$-bounded SO_4^{2-} concentrations exhibited a relatively gentle daily variation, with maximum values of 7 μg/m^3 (at 9:00), 8 μg/m^3 (at 12:00), 6 μg/m^3

(at 12:00), and 9 μg/m^3 (at 11:00) during the different seasons. The SOC concentrations showed a relatively gentle daily variation, with maximum values of 7 μg/m^3 (at 7:00), 7 μg/m^3 (at 11:00), 8 μg/m^3 (at 11:00), and 12 μg/m^3 (at 9:00).

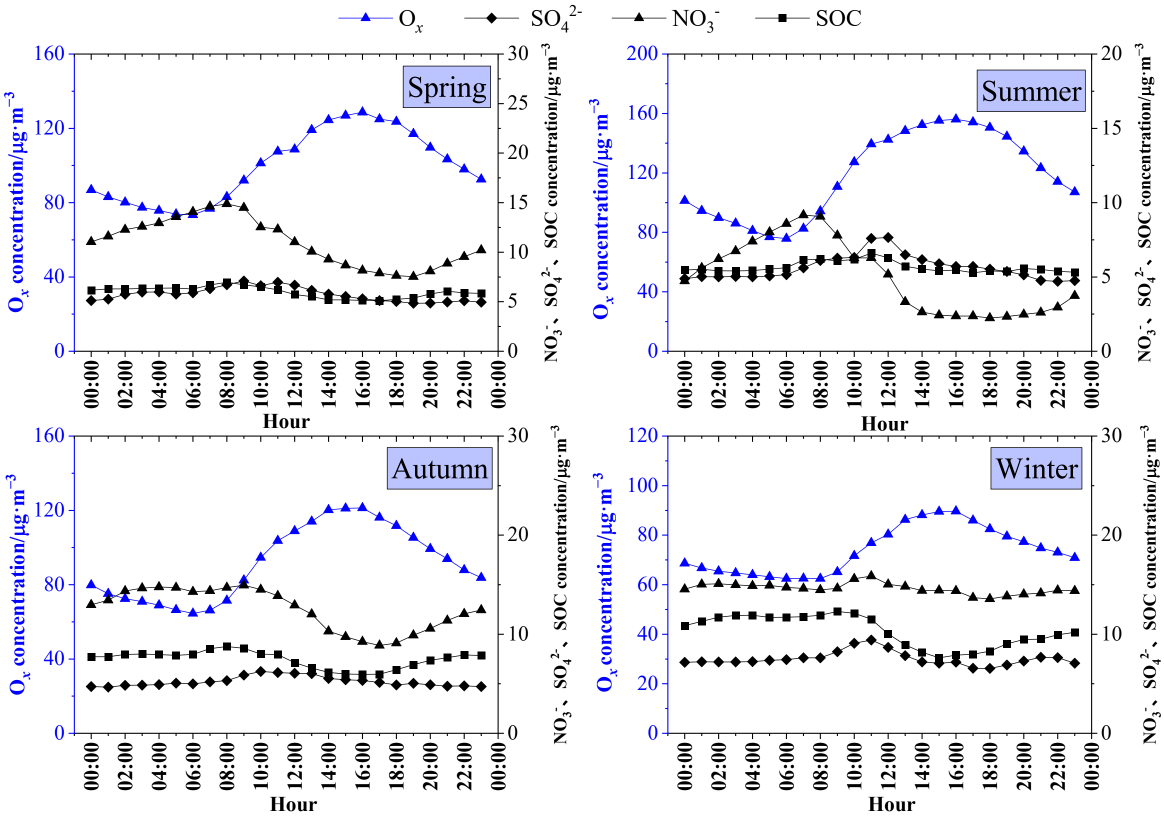

Figure 14. Distribution characteristics of O_x, PM$_{2.5}$-bounded NO_3^-, PM$_{2.5}$-bounded SO_4^{2-}, and SOC concentrations in Dongying during different seasons from 2022 to 2023.

3.3.2. Effects on Ozone and Atmospheric Oxidation at Night and the Next Day

In 2022 and 2023, the average nocturnal O_3 concentrations during NOE events in Dongying were 2 μg/m^3 and 1 μg/m^3 higher than the overall average nocturnal O_3 concentrations in 2022 and 2023, respectively. Conversely, the average nocturnal O_3 concentrations during NNOE events in Dongying in 2022 and 2023 were both 1 μg/m^3 lower than the overall average nocturnal O_3 concentrations in the same years. In 2022 and 2023, the average nocturnal ozone concentrations during NOE events in Dongying were 4 μg/m^3 and 2 μg/m^3 higher than those during NNOE events, respectively (Figure 15). The average nocturnal ozone concentrations during NOE events in January and June to October were higher than those during NNOE events. Compared to the NNOE events, the greater impact of the NOE events on the nocturnal ozone concentrations during the summer months may be attributed to more severe ozone pollution during the daytime in the summer. It is generally believed that NOE events are primarily influenced by atmospheric physical processes such as transport. From the perspective of horizontal transport, ozone concentrations in air masses are higher in the summer than in the winter; thus, upwind transport contributes to a greater increase in local ozone concentrations. From the perspective of vertical transport, higher residual layer ozone concentrations during the summer nights led to a more significant increase in the surface ozone concentrations. In January, the differences in ozone concentrations between NOE events and NNOE events may be attributed to the influence of other meteorological factors.

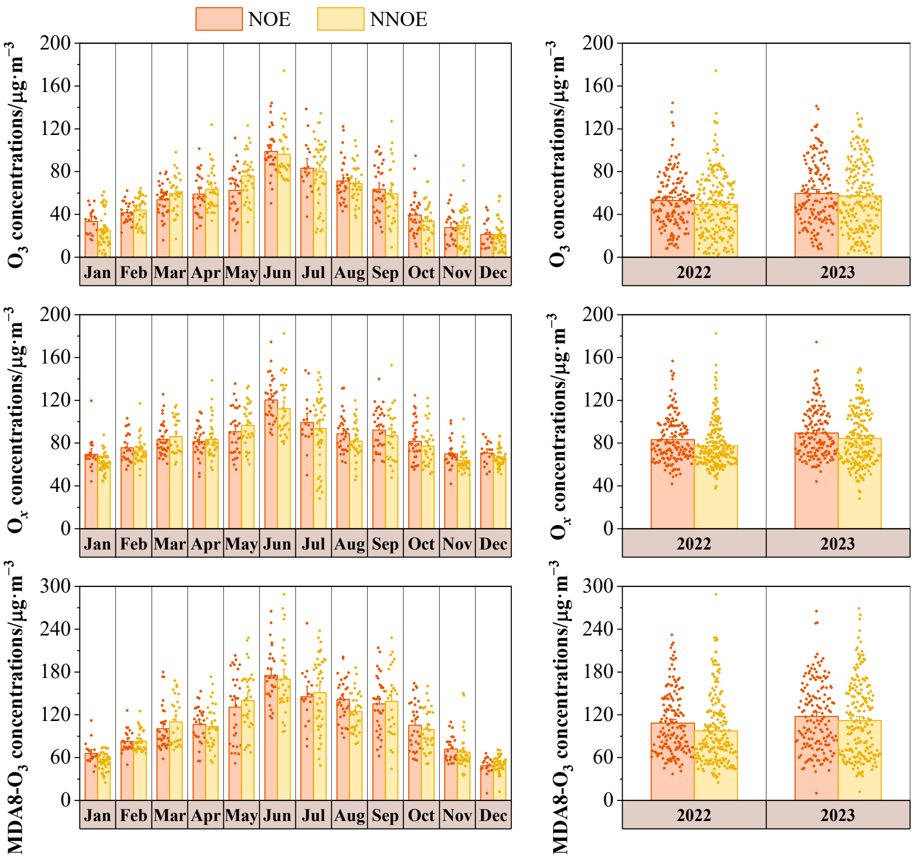

Figure 15. Difference in nocturnal O_3, O_x, and MDA8-O_3 of the same day during NOE events and NNOE events in Dongying from 2022 to 2023.

The average nocturnal O_x concentrations during the NOE events in Dongying in 2022 and 2023 were both 3 μg/m^3 higher than the overall average nocturnal O_x concentrations in the corresponding years. Conversely, the average nocturnal O_x concentrations during the NNOE events in Dongying in 2022 and 2023 were 3 μg/m^3 and 2 μg/m^3 lower than the overall average nocturnal O_x concentrations in the same years, respectively. In 2022 and 2023, the average nocturnal O_x concentrations during the NOE events in Dongying were 6 μg/m^3 and 5 μg/m^3 higher than those during NNOE events, respectively (Figure 15). The average nocturnal O_x concentrations during the NOE events in the summer, autumn, and winter were higher than those observed during the NNOE events. The differences in the average nocturnal O_x concentrations were higher in January and June, with a difference of 8 μg/m^3.

In 2022 and 2023, the average MDA8-O_3 concentrations on days with NOE events in Dongying were 11 μg/m^3 and 6 μg/m^3 higher than those during NNOE events, respectively (Figure 15). The average MDA8-O_3 concentrations on days with NOE events in January, April, June, August, October, and November were higher than those observed during NNOE events. The variations were observable in January (11 μg/m^3) and August (17 μg/m^3).

Consequently, in 2022 and 2023, the average nocturnal O_3 and O_x concentrations during the NOE events in Dongying were higher than the overall average nocturnal concentrations for the same years. Conversely, the average nocturnal O_3 and O_x concentrations during the NNOE events in Dongying were lower than the average nocturnal concentrations in 2022 and 2023. This indicates that NOE events contribute to an increase in nocturnal O_3 concentration and the atmospheric oxidizing capacity represented by O_x. The NOE events in Dongying from 2022 to 2023 exhibited enhancing effect on the nocturnal concentrations of O_3, O_x, and MDA8-O_3 on the same day, with increases of 3 μg/m^3, 6 μg/m^3, and 8 μg/m^3, respectively. This effect was observable during the summer and autumn.

In Dongying, during 2022 and 2023, the average ozone concentrations of the next day of NOE events were 10 μg/m^3 and 9 μg/m^3 higher than those during NNOE events, respectively (Figure 16). The average ozone concentrations on the next day of NOE events were distinctly higher than those during the NNOE events in every month except February and May. The differences were higher in June and July, both showing a variance of 13 μg/m^3. An increase in nocturnal ozone concentration may contribute to higher ozone levels on the following day [14,31,45,53]. This is primarily due to the elevated surface ozone concentrations during the night, resulting in a higher ozone background concentration and increasing the initial ozone concentration on the next day. Based on the observational data from 2022 to 2023 in Dongying, it was observed that the nighttime concentration of NO_2 in Dongying was lower in summer compared to the other seasons. The lower NO_2 concentration resulted in reduced nighttime ozone titration, leading to less ozone consumption during the night. Therefore, during the NOE events in the summer in Dongying, the ozone concentration on the next day was higher.

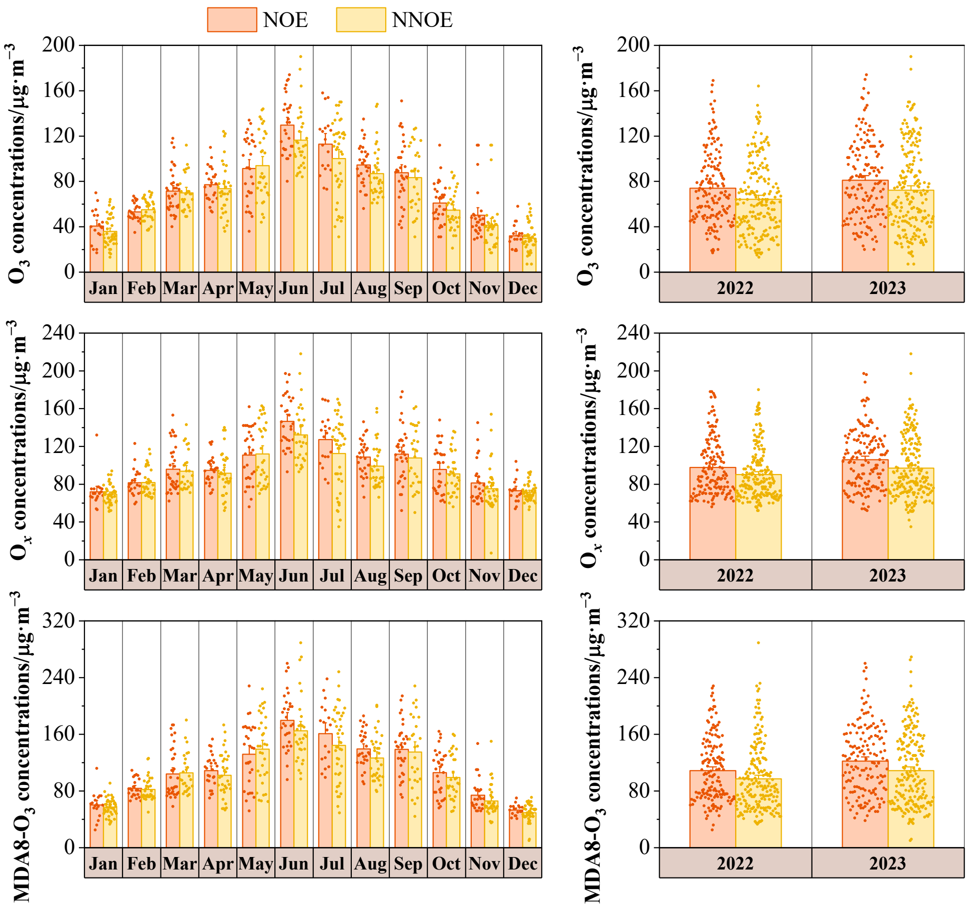

Figure 16. Differences in O_3, O_x, and MDA8-O_3 on the next day during NOE events and NNOE events in Dongying from 2022 to 2023.

In 2022 and 2023, the average O_x concentrations on the next day of NOE events were 8 μg/m^3 and 9 μg/m^3 higher than those during the NNOE events in Dongying, respectively (Figure 16). The average O_x concentrations on the next day of NOE events were higher than those during NNOE events in every month except for February and May. The differences were higher in June, July, and August, with differences of 14 μg/m^3, 15 μg/m^3, and 10 μg/m^3, respectively.

In 2022 and 2023, the average MDA8-O_3 concentrations of the next day of NOE events in Dongying were 12 μg/m^3 and 14 μg/m^3 higher than those during the NNOE events, respectively (Figure 16). The average MDA8-O_3 concentrations of the next day of NOE events were higher than those during the NNOE events in every month except March and May. The differences were higher from June to August, with differences of 15 μg/m^3, 17 μg/m^3, and 13 μg/m^3, respectively.

Overall, the NOE events in Dongying from 2022 to 2023 also exhibited a promoting effect on the O_3, O_x, and MDA8-O_3 of the next day, resulting in increases of 9 μg/m^3, 8 μg/m^3, and 13 μg/m^3, respectively. This effect was most obvious during the summer.

3.3.3. Effects on $PM_{2.5}$ Concentration and Secondary Components at Night and the Next Day

From 2022 to 2023, the correlations between the nocturnal O_x, $PM_{2.5}$, $PM_{2.5}$-bounded NO_3^-, SO_4^{2-}, and SOC during the different seasons in Dongying were analyzed (Figure 17). Significant correlations were observed between the nocturnal O_x and $PM_{2.5}$ as well as the SOC during different seasons in Dongying, with correlation coefficients ranging from 0.210 to 0.737. The correlation between the nocturnal O_x and $PM_{2.5}$-bounded NO_3^- was significant in both the summer and winter, with correlation coefficients of 0.351 and 0.781, respectively. Additionally, the correlation between nocturnal O_x and $PM_{2.5}$-bounded SO_4^{2-} was significant in the summer, autumn, and winter, with correlation coefficients of 0.385, 0.408, and 0.600, respectively. Thus, it can be observed that the increase in the nocturnal atmospheric oxidation capacity in Dongying had a certain impact on the $PM_{2.5}$ concentration and its secondary components. Based on the analysis in Section 3.3.2, the NOE events were found to increase the concentration of O_x, thereby enhancing the oxidation capacity of the atmosphere. Consequently, NOE events may have a certain impact on $PM_{2.5}$ concentrations and their secondary components. Hence, the effects of the NOE events on the concentrations of $PM_{2.5}$, $PM_{2.5}$-bounded NO_3^-, $PM_{2.5}$-bounded SO_4^{2-}, and SOC in Dongying from 2022 to 2023 were further analyzed in this study.

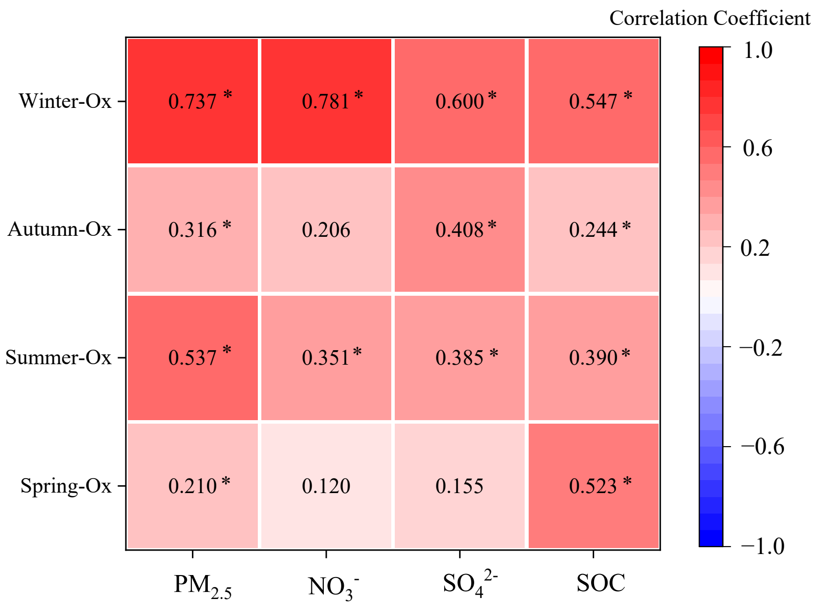

Figure 17. Correlations between O_x concentrations, $PM_{2.5}$, and $PM_{2.5}$-bounded components during different seasons of NOE events in Dongying from 2022 to 2023 (* indicates $p < 0.05$).

In 2022 and 2023, the average nocturnal $PM_{2.5}$ concentrations during the NOE events in Dongying exceeded the average nocturnal $PM_{2.5}$ concentrations for the respective years by 3 μg/m^3. Conversely, during the NNOE events in Dongying in 2022 and 2023, the average nocturnal $PM_{2.5}$ concentrations were 2 μg/m^3 and 1 μg/m^3 lower than the average nocturnal $PM_{2.5}$ concentrations for the same years, respectively. In 2022 and 2023, the average nocturnal $PM_{2.5}$ concentrations during the NOE events in Dongying were 5 μg/m^3 and 4 μg/m^3 higher than those during the NNOE events, respectively (Figure 18). The average nocturnal $PM_{2.5}$ concentrations during the NOE events were higher than those during the NNOE events in all months except for April and September. The differences were higher in November and December, with differences of 14 μg/m^3 and 32 μg/m^3, respectively.

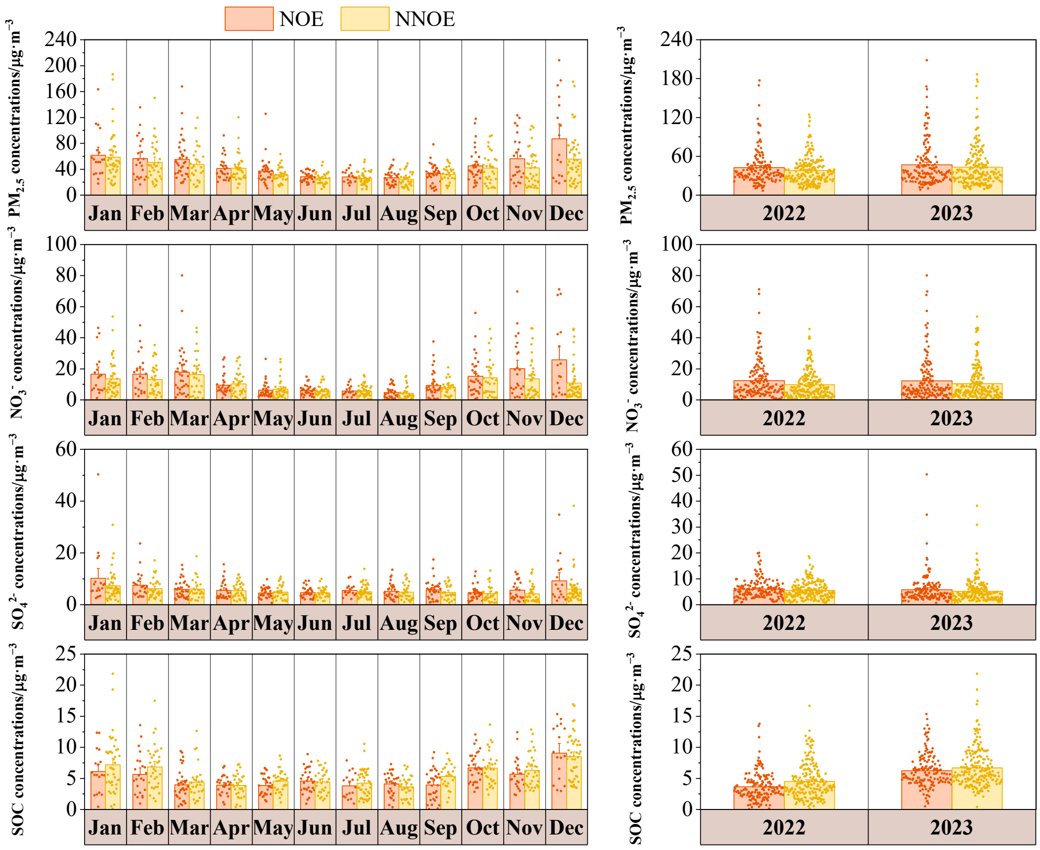

Figure 18. Differences in nocturnal $PM_{2.5}$, $PM_{2.5}$-bounded NO_3^-, SO_4^{2-}, and SOC during the NOE events and NNOE events in Dongying from 2022 to 2023.

The average nocturnal $PM_{2.5}$-bounded NO_3^- concentrations during the NOE events in Dongying in 2022 and 2023 exceeded the average nocturnal NO_3^- concentrations for the respective years by 1 μg/m^3. Conversely, during the NNOE events in Dongying in 2022 and 2023, the average nocturnal NO_3^- concentrations were both 1 μg/m^3 lower than the average nocturnal NO_3^- concentrations for the same years. In 2022 and 2023, the average nocturnal NO_3^- concentrations during the NOE events in Dongying were 3 μg/m^3 and 2 μg/m^3 higher than those during the NNOE events, respectively (Figure 18). The average nocturnal NO_3^- concentrations during the NOE events from January to March, November, and December were higher than those during the NNOE events. The differences were higher in November and December, with differences of 7 μg/m^3 and 15 μg/m^3, respectively.

The nocturnal $PM_{2.5}$-bounded SO_4^{2-} concentrations during the NOE events in Dongying in 2022 and 2023 were comparable to those during the NNOE events (Figure 18). The nocturnal SO_4^{2-} concentrations during the NOE events in January, February, November, and December were 3 μg/m^3, 1 μg/m^3, 1 μg/m^3, and 3 μg/m^3 higher than those during the NNOE events, respectively.

In 2022 and 2023, the average nocturnal SOC concentration during the NOE events in Dongying was comparable to those during the NNOE events, and sometimes even slightly lower than those during the NNOE events (Figure 18). This might be due to the complexity of the impact of nocturnal atmospheric oxidation on SOC, which could not be simply reflected by the average concentration of SOC. Further detailed research on the impact of NOE events on the secondary organic components in $PM_{2.5}$ is needed in the future.

In summary, the average nocturnal $PM_{2.5}$ and $PM_{2.5}$-bounded NO_3^- concentrations during the NOE events in Dongying were higher than the overall average nocturnal $PM_{2.5}$ and $PM_{2.5}$-bounded NO_3^- concentrations for the respective years. Conversely, the average nocturnal $PM_{2.5}$ and NO_3^- concentrations during the NNOE events in Dongying were lower than the overall average nocturnal $PM_{2.5}$ and NO_3^- for the respective years. This indicates that NOE events contribute to an increase in nocturnal $PM_{2.5}$ concentrations and $PM_{2.5}$-bounded NO_3^- concentrations. The NOE events exhibited a clear promoting effect on the nocturnal $PM_{2.5}$, $PM_{2.5}$-bounded NO_3^-, and SO_4^{2-} in Dongying from 2022 to 2023, with the most distinct impact during the winter. The NOE events did not demonstrate an obvious effect on the average nocturnal SOC concentration.

NOE events are more likely to increase $PM_{2.5}$ concentrations. He et al. (2023) observed a significant enhancement in nocturnal atmospheric oxidizing capacity and a notably higher $PM_{2.5}$ concentration during NOE events in Guangzhou, China. The increased oxidative capacity during NOE events promotes and accelerates nighttime chemical reactions, enhancing the generation of secondary pollutants such as $PM_{2.5}$ [31]. Additionally, Li et al. (2023) also observed that the increased nighttime ozone may enhance the conversion of $PM_{2.5}$-bounded NO_3^- through the promotion of heterogeneous hydrolysis of dinitrogen pentoxide, thereby influencing the long-term trend in nighttime NO_3^- concentrations [15].

The primary pathway for nocturnal $PM_{2.5}$-bounded NO_3^- formation is through the heterogeneous hydrolysis of dinitrogen pentoxide. Dinitrogen pentoxide is generated through the titration of NOx with ozone (NO_2 + O_3—NO_3 + O_2, NO_3 + NO_2—N_2O_5), which has a direct relationship with NOE events [54,55]. The formation pathway of nocturnal $PM_{2.5}$-bounded SO_4^{2-} is mainly through S(IV) + NO_2, SO_2 + aerosol, SO_2 + O_2 (metal ion catalysis). Nocturnal NO_2 and O_3 can generate O_2, facilitating the pathway of SO_2 + O_2 to produce SO_4^{2-}. However, the contribution of the SO_2 + O_2 pathway to SO_4^{2-} generation is relatively low (about 2%) [56,57]. Therefore, compared to $PM_{2.5}$-bounded NO_3^-, the impact of NOE events on SO_4^{2-} generation is relatively small. SOC species are more complex and primarily formed through reactions between nocturnal oxidants such as O_3, NO_3 radicals, and VOCs. An increase in nighttime ozone concentration elevates nighttime atmospheric oxidants, but further exploration is needed regarding its interaction with VOCs.

The NOE events had obvious effects on nocturnal $PM_{2.5}$, $PM_{2.5}$-bounded NO_3^- and SO_4^{2-}. Therefore, the differences between nocturnal NOR and SOR during NOE events and NNOE events were further analyzed in this study (Figure 19).

The nocturnal NOR values during the NOE events in 2022 and 2023 were 0.006 and 0.005 higher than those during the NNOE events in Dongying, respectively (Figure 19). The nocturnal NOR values during the NOE events in January, February, October, November and December were 0.03, 0.006, 0.02, 0.01, and 0.09 higher than those during the NNOE events, respectively. This was consistent with the effects of NOE events on $PM_{2.5}$-bounded NO_3^- concentrations, indicating that NOE events may affect the concentration of NO_3^- by affecting the oxidation of nocturnal NO_2.

The nocturnal SOR during the NOE events in 2022 and 2023 were 0.02 higher than those during the NNOE events in Dongying (Figure 19). Specifically, the nocturnal SOR during the NOE events in January, February, June, July, September, October, November, and December were 0.03, 0.01, 0.04, 0.02, 0.04, 0.03, 0.06, and 0.10 higher than those during the NNOE events, respectively. This pattern aligns with the observed impact of NOE events on SO_4^{2-} concentrations, indicating that NOE events may affect the concentration of SO_4^{2-} by affecting the oxidation of nocturnal SO_2.

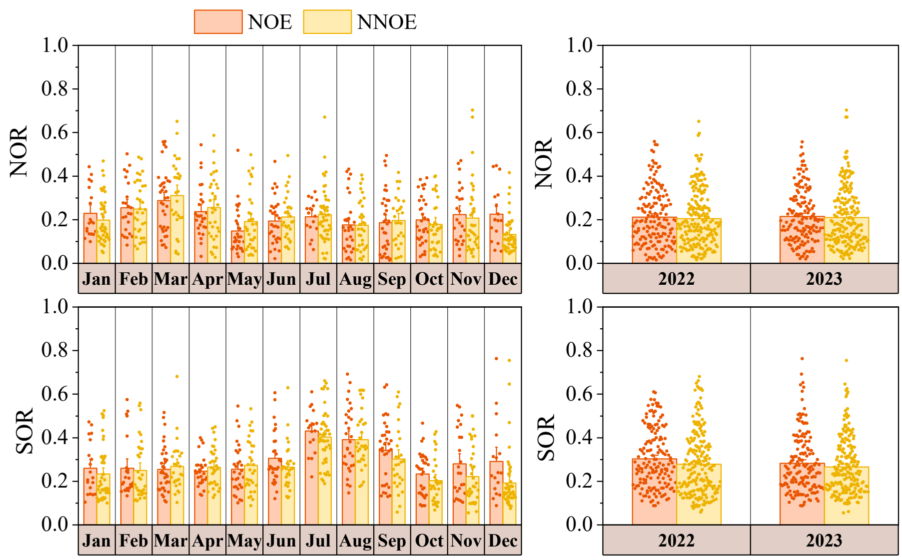

Figure 19. Differences in nocturnal NOR and SOR during the NOE events and NNOE events in Dongying from 2022 to 2023.

In 2022 and 2023, the average $PM_{2.5}$ concentration on the next day of NOE events in Dongying was generally comparable to those during the NNOE events (Figure 20). The average $PM_{2.5}$ concentration of the next day of NOE events was slightly higher than those of the NNOE events in May, June, July, August, October, and December, with a difference of about 3 $\mu g/m^3$.

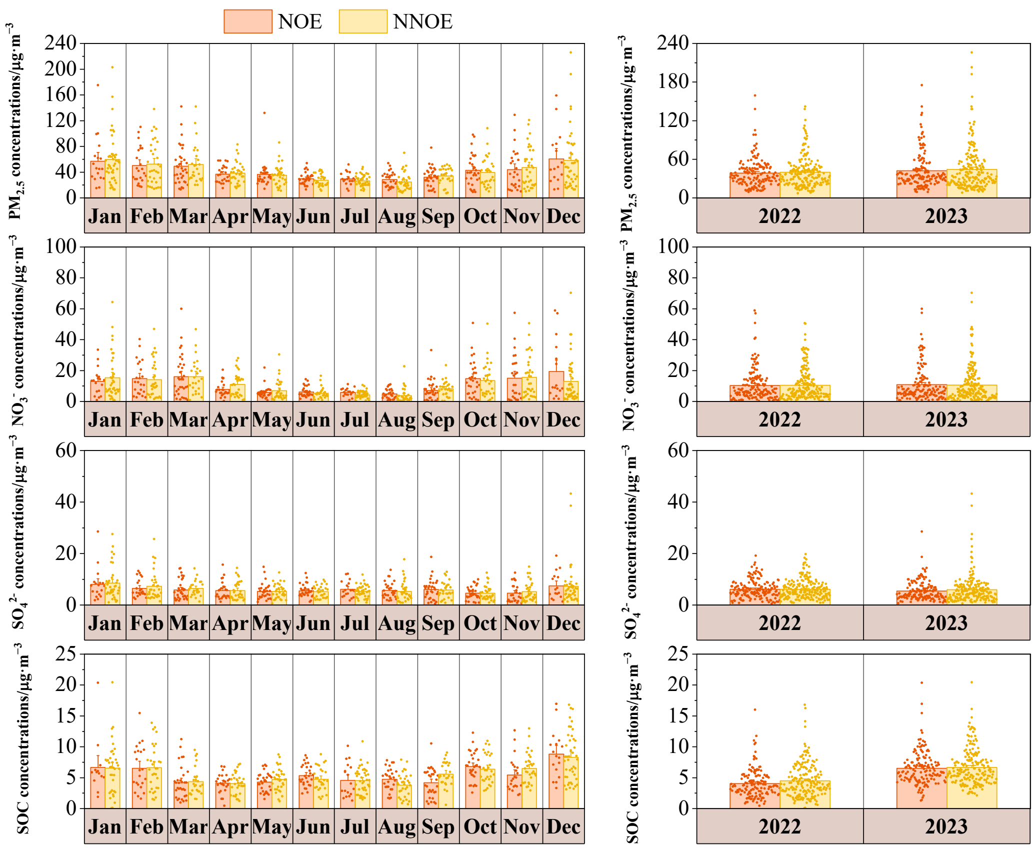

Figure 20. Differences in $PM_{2.5}$, $PM_{2.5}$-bounded NO_3^-, SO_4^{2-}, and SOC concentrations of the next day during the NOE events and NNOE events in Dongying from 2022 to 2023.

In 2022 and 2023, the average $PM_{2.5}$-bounded NO_3^- concentration on the next day of NOE events in Dongying was generally comparable to those during NNOE events (Figure 20). The average concentration of NO_3^- on the next day of the NOE events in December was 6 $\mu g/m^3$ higher than that during the NNOE event, and there were no significant differences in the other months. Hence, the NOE events had a noticeable impact on the average concentration of $PM_{2.5}$-bounded NO_3^- on the following day in December but did not conspicuously affect the other months.

Regarding the annual and monthly average concentrations of $PM_{2.5}$-bounded SO_4^{2-} and SOC on the next day after the NOE and NNOE events, the differences in concentrations were relatively small (all less than 1 $\mu g/m^3$) (Figure 20). Furthermore, a non-parametric test (Mann–Whitney test) was employed for verification, and the results indicated no significant differences in the $PM_{2.5}$-bounded SO_4^{2-} concentrations between the second day after the NOE and NNOE events (statistical value Z = -0.07678, $p > 0.05$). Similarly, there was no significant difference in the SOC concentrations between the second day after the NOE and NNOE events (statistical value Z = -1.33106, $p > 0.05$).

In summary, the NOE events showed no obvious effects on the $PM_{2.5}$, $PM_{2.5}$-bounded NO_3^-, $PM_{2.5}$-bounded SO_4^{2-}, and SOC concentrations of the following day in Dongying from 2022 to 2023. On the following day after NOE events, O_3 undergoes a series of complex atmospheric physical and chemical processes (such as deposition, transport, and photochemical reactions), resulting in significant concentration changes. Therefore, the impact of NOE events on the concentrations of $PM_{2.5}$, $PM_{2.5}$-bounded NO_3^-, $PM_{2.5}$-bounded SO_4^{2-}, and SOC on the following day may be smaller. Further quantitative research is needed to determine the influence of NOE events on the generation of secondary pollutants on the following day.

4. Conclusions

(1) From 2022 to 2023, the annual average nocturnal ozone concentration in Dongying increased from 51 $\mu g/m^3$ to 59 $\mu g/m^3$. The different percentile values of the nocturnal ozone concentrations also showed an increase in these two years, with the most notable increases observed in the high and middle percentiles. The nocturnal ozone concentrations were higher during the ozone pollution seasons and lower during the non-ozone pollution seasons. Compared with 2022, the nocturnal ozone concentration increased most apparently in the spring and summer of 2023.

(2) For 2022 and 2023, the annual average frequencies of NOE events in Dongying were 44% and 43%, respectively. The frequency of NOE events was higher in the spring, summer, and autumn and lower in the winter. The diurnal variation characteristics of the frequency of NOE events were generally similar in both 2022 and 2023, featuring a higher frequency from 2:00 to 4:00 and a lower frequency from 21:00 to 1:00 the next day.

(3) The NOE events exhibited an obvious promoting effect on nocturnal O_3, O_x, and MDA8-O_3 on the same day in Dongying from 2022 to 2023, with a more noticeable increase observed during the summer and autumn. The NOE events also had a distinct effect on the O_3, O_x, and MDA8-O_3 of the next day, with the most conspicuous effect observed in summer. In terms of government control, it is essential to assess the ozone pollution status of the next day based on the characteristics of nocturnal ozone changes. Moreover, the NOE events had evident effects on the nocturnal concentrations of $PM_{2.5}$ and $PM_{2.5}$-bounded NO_3^- and SO_4^{2-}, with the impact being most apparent in the winter. However, the NOE events had no conspicuous impact on the concentrations of $PM_{2.5}$, $PM_{2.5}$-bounded NO_3^-, $PM_{2.5}$-bounded SO_4^{2-}, and SOC on the next day.

(4) NOE events have distinct effects on the concentrations of O_3, O_x, MDA8-O_3, $PM_{2.5}$, and $PM_{2.5}$-bounded NO_3^- and SO_4^{2-}. This implies that NOE events can improve atmospheric oxidation capacity and promote the formation of $PM_{2.5}$ and its secondary components, which have a certain impact on air quality. Consequently, increased

attention should be given to the occurrence of NOE events and the challenges brought by NOE to the coordinated control of $PM_{2.5}$ and O_3. More sophisticated methods should be employed to investigate the impact of NOE on atmospheric oxidation capacity and $PM_{2.5}$, along with its secondary components in the future. Additionally, given the increasing prevalence of human nocturnal activities, it is imperative to delve into the repercussions of NOE on human health and biological growth.

Author Contributions: Conceptualization, C.A. and H.L.; data curation, F.S., J.L. and L.T.; formal analysis, Y.Y., X.G., X.Y. and Y.J.; funding acquisition, R.G. and H.L.; methodology, C.A., Y.Y. and H.L.; project administration, Y.J. and F.B.; supervision, H.L.; writing—original draft, C.A.; writing—review and editing, C.A. and H.L. All authors have read and agreed to the published version of the manuscript.

Funding: This work was supported by the Ministry of Ecology and Environment of China under the project (DQGG202121) and the Dongying Ecological and Environmental Bureau (2021DFKY-0779).

Institutional Review Board Statement: Not applicable.

Informed Consent Statement: Not applicable.

Data Availability Statement: The data presented in this study are available on request from the corresponding author. The data are not publicly available due to privacy.

Conflicts of Interest: The author Luyao Tan was employed by the company Ltd. of Shandong Environmental Protection Industry Corp. The paper reflects the views of the scientists, and not the company. The remaining authors declare that the research was conducted in the absence of any commercial or financial relationships that could be construed as potential conflicts of interest.

References

1. Wang, T.; Xue, L.; Brimblecombe, P.; Lam, Y.F.; Li, L.; Zhang, L. Ozone pollution in China: A review of concentrations, meteorological influences, chemical precursors, and effects. *Sci. Total Environ.* **2017**, *575*, 1582–1596. [CrossRef]
2. Tan, Z.; Ma, X.; Lu, K.; Jiang, M.; Zou, Q.; Wang, H.; Zeng, L.; Zhang, Y. Direct evidence of local photochemical production driven ozone episode in Beijing: A case study. *Sci. Total Environ.* **2021**, *800*, 148868. [CrossRef]
3. Zeren, Y.; Zhou, B.; Zheng, Y.; Jiang, F.; Lyu, X.; Xue, L.; Wang, H.; Liu, X.; Guo, H. Does ozone pollution share the same formation mechanisms in the bay areas of China? *Environ. Sci. Technol.* **2022**, *56*, 14326–14337. [CrossRef]
4. Liu, Y.; Geng, G.; Cheng, J.; Liu, Y.; Xiao, Q.; Liu, L.; Shi, Q.; Tong, D.; He, K.; Zhang, Q. Drivers of increasing ozone during the two phases of Clean Air Actions in China 2013–2020. *Environ. Sci. Technol.* **2023**, *57*, 8954–8964. [CrossRef]
5. Lu, X.; Hong, J.; Zhang, L.; Cooper, O.R.; Schultz, M.G.; Xu, X.; Wang, T.; Gao, M.; Zhao, Y.; Zhang, Y. Severe surface ozone pollution in China: A global perspective. *Environ. Sci. Technol. Lett.* **2018**, *5*, 487–494. [CrossRef]
6. Strode, S.A.; Ziemke, J.R.; Oman, L.D.; Lamsal, L.N.; Olsen, M.A.; Liu, J. Global changes in the diurnal cycle of surface ozone. *Atmos. Environ.* **2019**, *199*, 323–333. [CrossRef]
7. Bernier, C.; Wang, Y.; Estes, M.; Lei, R.; Jia, B.; Wang, S.C.; Sun, J. Clustering surface ozone diurnal cycles to understand the impact of circulation patterns in Houston, TX. *J. Geophys. Res. Atmos.* **2019**, *124*, 13457–13474. [CrossRef]
8. Lin, J.; Youn, D.; Liang, X.; Wuebbles, D. Global model simulation of summertime U.S. ozone diurnal cycle and its sensitivity to PBL mixing, spatial resolution, and emissions. *Atmos. Environ.* **2008**, *42*, 8470–8483. [CrossRef]
9. Xia, N.; Du, E.; Guo, Z.; Vries, W.D. The diurnal cycle of summer tropospheric ozone concentrations across Chinese cities: Spatial patterns and main drivers. *Environ. Pollut.* **2021**, *286*, 117547. [CrossRef]
10. Xu, J.; Huang, X.; Wang, N.; Li, Y.; Ding, A. Understanding ozone pollution in the Yangtze River Delta of eastern China from the perspective of diurnal cycles. *Sci. Total Environ.* **2021**, *752*, 141928. [CrossRef]
11. Talbot, R.; Mao, H.; Sive, B. Diurnal characteristics of surface level O_3 and other important trace gases in New England. *J. Geophys. Res. Atmos.* **2005**, *110*, D09307. [CrossRef]
12. Zhu, X.; Ma, Z.; Li, Z.; Wu, J.; Guo, H.; Yin, X.; Ma, X.; Qiao, L. Impacts of meteorological conditions on nocturnal surface ozone enhancement during the summertime in Beijing. *Atmos. Environ.* **2020**, *225*, 117368. [CrossRef]
13. He, Y.; Wang, H.; Wang, H.; Xu, X.; Li, Y.; Fan, S. Meteorology and topographic influences on nocturnal ozone increase during the summertime over Shaoguan, China. *Atmos. Environ.* **2021**, *256*, 118459. [CrossRef]
14. He, C.; Lu, X.; Wang, H.; Wang, H.; Li, Y.; He, G.; He, Y.; Wang, Y.; Zhang, Y.; Liu, Y.; et al. The unexpected high frequency of nocturnal surface ozone enhancement events over China: Characteristics and mechanisms. *Atmos. Chem. Phys.* **2022**, *22*, 15243–15261. [CrossRef]

15. Li, X.; Ren, J.; Huang, R.; Chen, L.; Li, Y.; Qiao, X.; Cheng, Y.; Zhao, B.; Yin, D.; Gao, D.; et al. The aggravation of summertime nocturnal ozone pollution in China and its potential impact on the trend of nitrate aerosols. *Geophys. Res. Lett.* **2023**, *50*, e2023GL103242. [CrossRef]
16. Eliasson, I.; Thorsson, S.; Andersson-Sköld, Y. Summer nocturnal ozone maxima in Göteborg, Sweden. *Atmos. Environ.* **2003**, *37*, 2615–2627. [CrossRef]
17. Salmond, J.A.; McKendry, I.G. Secondary ozone maxima in a very stable nocturnal boundary layer: Observations from the Lower Fraser Valley, BC. *Atmos. Environ.* **2002**, *36*, 5771–5782. [CrossRef]
18. Agathokleous, E.; Feng, Z.; Sicard, P. Surge in nocturnal ozone pollution. *Science* **2023**, *382*, 1131. [CrossRef]
19. Alduwais, A.K.; Dasari, H.P.; Karumuri, R.K.; Gandham, H.; Alharbi, B.H.; Ashok, K.; Hoteit, I. Transport mechanisms of nocturnal surface ozone over Riyadh, Kingdom of Saudi Arabia. *Atmos. Environ.* **2023**, *313*, 120069. [CrossRef]
20. Wang, J.; Wang, D.; Ge, B.; Lin, W.; Ji, D.; Pan, X.; Li, J.; Wang, Z. Increase in daytime ozone exposure due to nighttime accumulation in a typical city in eastern China during 2014–2020. *Atmos. Pollut. Res.* **2022**, *13*, 101387. [CrossRef]
21. Wang, H.; Wang, H.; Lu, X.; Lu, K.; Zhang, L.; Tham, Y.J.; Shi, Z.; Aikin, K.; Fan, S.; Brown, S.S.; et al. Increased night-time oxidation over China despite widespread decrease across the globe. *Nat. Geosci.* **2023**, *16*, 217–223. [CrossRef]
22. Lloyd, K.L.; Davis, D.D.; Marini, R.P.; Decoteau, D.R. Effects of nighttime ozone treatment at ambient concentrations on sensitive and resistant snap bean genotypes. *J. Am. Soc. Hortic.* **2018**, *143*, 23–33. [CrossRef]
23. Agathokleous, E.; Feng, Z.; Oksanen, E.; Sicard, P.; Wang, Q.; Saitanis, C.J.; Araminiene, V.; Blande, J.D.; Hayes, F.; Calatayud, V.; et al. Ozone affects plant, insect, and soil microbial communities: A threat to terrestrial ecosystems and biodiversity. *Sci. Adv.* **2020**, *6*, eabc1176. [CrossRef] [PubMed]
24. Wu, Y.; Chen, W.; You, Y.; Xie, Q.; Jia, S.; Wang, X. Quantitative impacts of vertical transport on the long-term trend of nocturnal ozone increase over the Pearl River Delta region during 2006–2019. *Atmos. Chem. Phys.* **2023**, *23*, 453–469. [CrossRef]
25. Meng, K.; Zhao, T.; Xu, X.; Hu, Y.; Zhao, Y.; Zhang, L.; Pang, Y.; Ma, X.; Bai, Y.; Zhao, Y.; et al. Anomalous surface O_3 changes in North China Plain during the northwestward movement of a landing typhoon. *Sci. Total Environ.* **2022**, *820*, 153196. [CrossRef] [PubMed]
26. Ouyang, S.; Deng, T.; Liu, R.; Chen, J.; He, G.; Leung, J.C.-H.; Wang, N.; Liu, S.C. Impact of a subtropical high and a typhoon on a severe ozone pollution episode in the Pearl River Delta, China. *Atmos. Chem. Phys.* **2022**, *22*, 10751–10767. [CrossRef]
27. Zhao, D.; Xin, J.; Wang, W.; Jia, D.; Wang, Z.; Xiao, H.; Liu, C.; Zhou, J.; Tong, L.; Ma, Y.; et al. Effects of the sea-land breeze on coastal ozone pollution in the Yangtze River Delta, China. *Sci. Total Environ.* **2022**, *807*, 150306. [CrossRef]
28. Wang, Y.; Wang, H.; Wang, W. A Stratospheric intrusion-influenced ozone pollution episode associated with an intense horizontal-trough event. *Atmosphere* **2020**, *11*, 164. [CrossRef]
29. Ni, Z.-Z.; Luo, K.; Gao, X.; Gao, Y.; Fan, J.-R.; Fu, J.S.; Chen, C.-H. Exploring the stratospheric source of ozone pollution over China during the 2016 Group of Twenty summit. *Atmos. Pollut. Res.* **2019**, *10*, 1267–1275. [CrossRef]
30. He, G.; He, C.; Wang, H.; Miao, S.; Liu, C.; Wang, Y.; Liu, N.; Cao, T.; Deng, T.; Wu, D.; et al. Nocturnal ground-level ozone enhancement over the Pearl River Estuary: Two case studies based on vertical observations. *Acta Sci. Circumstantiae* **2023**, *43*, 87–96. [CrossRef]
31. He, C.; He, G.; Liu, C.; Wang, H.; Chen, X.; Liu, N.; Wang, H.; Lu, X.; Fan, S. Characteristics of nocturnal ozone enhancement events and a case study of horizontal transport in Guangzhou during warm season. *Acta Sci. Circumstantiae* **2023**, *43*, 76–86. [CrossRef]
32. Zhao, M.; Shen, H.; Chen, T.; Li, J.; Sun, Z.; Ji, Y.; Xue, L.; Li, H.; Wang, W.; Shang, F. Characteristics and sensitivity analysis of ozone in the representative city of the Yellow River Delta in summer. *Res. Environ. Sci.* **2022**, *35*, 1351–1361. [CrossRef]
33. Du, X.; Zhang, L.; Liang, H. Variation characteristics and correlation analysis of air quality index and acid rain in Dongying City. *J. Environ. Eng. Technol.* **2021**, *11*, 33–40. [CrossRef]
34. Ji, Y.; An, C.; Tang, J.; Li, J.; Yan, X.; Gao, X.; Chu, W.; Zhong, X.; Shang, F.; Li, J.; et al. Causes investigation of $PM_{2.5}$ and O_3 complex pollution in a typical coastal city in the Bohai Bay Region of China in autumn: Based on one-month continuous intensive observation and model simulation. *Atmosphere* **2024**, *15*, 73. [CrossRef]
35. An, C.; Ji, Y.; Chu, W.; Yan, X.; Bi, F.; Gao, Y.; Xue, L.; Shang, F.; Li, J.; Li, H. Spatiotemporal distribution characteristics of ground-level-ozone and its relationship with meteorological conditions in a representative city in the Bohai Rim from 2017 to 2022. *Environ. Sci.* **2024**, *8*. [CrossRef]
36. Huang, B.; Huang, Y.; Bao, S. A new exploration on the strategic functions of central cities from the perspective of the rise of the Yellow River Delta. *Truth Seek.* **2013**, *S2*, 141–143.
37. Ismail, A.A.K.H. Prediction of global solar radiation from sunrise duration using regression functions. *Kuwait J. Sci.* **2022**, *49*, 1–8. [CrossRef]
38. Zeng, Z.; Wang, Z.; Gui, K.; Yan, X.; Gao, M.; Luo, M.; Geng, H.; Liao, T.; Li, X.; An, J.; et al. Daily global solar radiation in China estimated from high-density meteorological observations: A random forest model framework. *Earth Space Sci.* **2020**, *7*, e2019EA001058. [CrossRef]
39. Kaplanis, S.N. New methodologies to estimate the hourly global solar radiation; Comparisons with existing models. *Renew. Energy* **2006**, *31*, 781–790. [CrossRef]
40. Ayodele, T.R.; Ogunjuyigbe, A.S.O.; Monyei, C.G. On the global solar radiation prediction methods. *J. Renew. Sustain. Energy* **2016**, *8*, 023702. [CrossRef]

41. Mullen, R.; Marshall, L.; McGlynn, B. A beta regression model for improved solar radiation predictions. *J. Appl. Meteorol. Clim.* **2013**, *52*, 1938. [CrossRef]
42. Jia, D.; Yang, L.; Lv, T.; Liu, W.; Gao, X.; Zhou, J. Evaluation of machine learning models for predicting daily global and diffuse solar radiation under different weather/pollution conditions. *Renew. Energy* **2022**, *187*, 896–906. [CrossRef]
43. Mughal, S.N.; Sood, Y.R.; Jarial, R.K. A neural network-based time-series model for predicting global solar radiations. *IETE J. Res.* **2021**, *69*, 3418–3430. [CrossRef]
44. Chu, W.; Li, L.; Li, H.; Zhang, Y.; Chen, Y.; Zhi, G.; Yang, X.; Ji, Y.; Chai, F. Atmospheric oxidation capacity and its impact on the secondary inorganic components of $PM_{2.5}$ in recent years in Beijing: Enlightenment for $PM_{2.5}$ pollution control in the Future. *Atmosphere* **2023**, *14*, 1252. [CrossRef]
45. An, C.; Li, H.; Ji, Y.; Chu, W.; Yan, X.; Chai, F. A review on nocturnal surface ozone enhancement: Characterization, formation causes, and atmospheric chemical effects. *Sci. Total Environ.* **2024**, *921*, 170731. [CrossRef] [PubMed]
46. He, G.; He, C.; Wang, H.; Lu, X.; Pei, C.; Qiu, X.; Liu, C.; Wang, Y.; Liu, N.; Zhang, J.; et al. Nighttime ozone in the lower boundary layer: Insights from 3-year tower-based measurements in South China and regional air quality modeling. *Atmos. Chem. Phys.* **2023**, *23*, 13107–13124. [CrossRef]
47. Yang, H.; Lu, C.; Hu, Y.; Chan, P.-W.; Li, L.; Zhang, L. Effects of horizontal transport and vertical mixing on nocturnal ozone pollution in the Pearl River Delta. *Atmosphere* **2022**, *13*, 1318. [CrossRef]
48. Shao, Y.; Zhang, J.; Ishizuka, M.; Mikami, M.; Leys, J.; Huang, N. Dependency of particle size distribution at dust emission on friction velocity and atmospheric boundarylayer stability. *Atmos. Chem. Phys.* **2020**, *20*, 12939–12953. [CrossRef]
49. Shan, W.; Yin, Y.; Zhang, J.; Ding, Y. Observational study of surface ozone at an urban site in East China. *Atmos. Res.* **2008**, *89*, 252–261. [CrossRef]
50. Yusoff, M.F.; Latif, M.T.; Juneng, L.; Khan, M.F.; Ahamad, F.; Chung, J.X.; Mohtar, A.A.A. Spatio-temporal assessment of nocturnal surface ozone in Malaysia. *Atmos. Environ.* **2019**, *207*, 105–116. [CrossRef]
51. Jia, S.; Xu, X.; Lin, W.; Wang, Y.; He, X.; Zhang, H. Increased mixing ratio of surface ozone by nighttime convection process over the North China Plain. *J. Appl. Meteor. Sci.* **2015**, *26*, 280–290. [CrossRef]
52. Chen, Z.; Liu, J.; Qie, X.; Cheng, X.; Shen, Y.; Yang, M.; Jiang, R.; Liu, X. Transport of substantial stratospheric ozone to the surface by a dying typhoon and shallow convection. *Atmos. Chem. Phys.* **2022**, *22*, 8221–8240. [CrossRef]
53. Sullivan, J.; Rabenhorst, S.; Dreessen, J.; McGee, T.; Delgado, R.; Twigg, L.; Sumnicht, G. Lidar observations revealing transport of O_3 in the presence of a nocturnal low-level jet: Regional implications for "next-day" pollution. *Atmos. Environ.* **2017**, *158*, 160–171. [CrossRef]
54. Zhai, T.; Lu, K.; Wang, H.; Lou, S.; Chen, X.; Hu, R.; Zhang, Y. Elucidate the formation mechanism of particulate nitrate based on direct radical observations in the Yangtze River Delta summer 2019. *Atmos. Chem. Phys.* **2023**, *23*, 2379–2391. [CrossRef]
55. Wang, H.; Lu, K.; Tan, Z.; Chen, X.; Liu, Y.; Zhang, Y. Formation mechanism and control strategy for particulate nitrate in China. *J. Environ. Sci.* **2023**, *123*, 476–486. [CrossRef]
56. Xue, J.; Yuan, Z.; Griffith, S.; Yu, X.; Lau, A.; Yu, J. Sulfate formation enhanced by a cocktail of high NO_x,SO_2, particulate matter, and droplet pH during Haze-Fog events in megacities in China: An observation-based modeling investigation. *Environ. Sci. Technol.* **2023**, *123*, 476–486. [CrossRef]
57. Ye, C.; Lu, K.; Song, H.; Mu, Y.; Chen, J.; Zhang, Y. A critical review of sulfate aerosol formation mechanisms during winter polluted periods. *J. Environ. Sci.* **2023**, *123*, 387–399. [CrossRef]